E-64

ARR No. E5B16

NATIONAL ADVISORY COMMITTEE FOR AERONAUTICS

WARTIME REPORT

ORIGINALLY ISSUED

March 1945 as
Advance Restricted Report E5B16

FLIGHT TESTS OF A P-63A-1 AIRPLANE WITH AN ELECTRIC TORQUEMETER

By J. Cary Nettles and Morgan P. Hanson

Aircraft Engine Research Laboratory
Cleveland, Ohio

NACA

WASHINGTON

E-64

NATIONAL ADVISORY COMMITTEE FOR AERONAUTICS

ADVANCE RESTRICTED REPORT

FLIGHT TESTS OF A P-63A-1 AIRPLANE WITH AN ELECTRIC TORQUEMETER

By J. Cary Nettles and Morgan P. Hanson

SUMMARY

The NACA has developed an electric torquemeter that was used to measure the power of an Allison V-1710-93 engine installed in a Bell P-63A-1 airplane.

Results of maximum-available-power tests made in flight at density altitudes ranging from about 23,000 to 31,000 feet showed good agreement between the measured maximum power output and the maximum power shown on the engine manufacturer's calibration chart. Results of other tests at a constant density altitude of 18,900 feet and at variable manifold pressure showed that greater manifold pressures were measured in flight for a given power than are indicated by the calibration chart.

INTRODUCTION

When aircraft-engine power is measured in flight, a much more complete understanding of the performance characteristics of the airplane is possible. The specific fuel consumption and the power required to fly become known and comparisons can be made at various engine speeds in order to establish the most favorable conditions of operation for flight at any given airspeed and altitude.

It is also desirable to be able to verify charted predictions (reference 1) of engine performance at altitude based upon sea-level tests or upon tests under simulated altitude conditions. The three main purposes for making power measurements in flight are:

(a) To aid in engine development

(b) To assist in establishing bases for predicting engine performance at altitude

(c) To distinguish between engine and airframe performance

The measurement of the torque of radial engines with planetary reduction gears has been so advanced that certain production engines are regularly being equipped with a hydraulically balanced piston, which restrains a fixed gear of the system. This mechanism, however, cannot be readily used on engines having the propeller mounted directly upon the crankshaft or on in-line engines with spur-gear reduction systems.

An alternate, though less accurate, method of determining power in flight (reference 2) by use of performance charts that give the power output of an engine for various conditions of altitude, manifold pressure, and engine speed has been resorted to when torquemeters were not available. The charted power must be corrected for variations in air temperature from standard and is subject to error because of ram, differences in mixture strength, general condition of the engine, the use of jet exhaust stacks, and other installation factors.

An electric torquemeter that is adaptable to any type of engine has been developed by the Engine Research Division of the NACA Aircraft Engine Research Laboratory. This apparatus employs resistance-wire strain gages arranged as a Wheatstone bridge and mounted directly upon the engine shaft so that the unbalance of the bridge circuit is proportional to the torsional strain in the shaft.

As part of a program of investigation of the Allison V-1710-93 engine installation in the Bell P-63A-1 airplane, an electric torquemeter was used to measure the power of this engine in flight. The calibrations and flight tests covered by this paper were made during April and May 1944 by the Flight Research Division at Cleveland, Ohio. The flight data were taken from 10 flight-test runs, 5 of which were made at maximum engine power and at density altitudes from 23,000 to 31,000 feet and the other 5 of which were made at a constant density altitude of about 18,900 feet with varying manifold pressure.

THE NACA ELECTRIC TORQUEMETER

Construction

The electric torquemeter used in these tests utilizes four resistance-wire strain gages similar to those described in reference 3. These strain gages are attached to a shaft at equal intervals around the circumference. (See fig. 1.) The wires of the strain gages make angles of 45° with the longitudinal axis of the shaft. The adjacent strain gages have spirals of opposite hand. Thus, when a torque is applied to the shaft, two strain gages will be subjected to tension and the other two will undergo compression.

The four strain gages are electrically connected to form a Wheatstone bridge. The wire in the gages changes its resistance in accordance with the changes in length (reference 3) caused by the applied torque. When the torque is zero and the bridge is balanced, no current will flow in the meter circuit if a voltage is impressed at opposite corners of the bridge. A torque applied to the shaft, however, will unbalance the bridge and a current will flow that is proportional to the strain in the shaft. Thus, for strains to which Hooke's law applies, a linear relation exists between the meter current and the applied torque.

Temperature changes, variations in thrust load, and bending of the shaft are selfcompensating within the bridge circuit and cause only slight electrical unbalance, the effect of which is within the over-all accuracy of the device. A maximum drift of the meter zero observed between the beginning and the end of any one flight was 2 microamperes. The effect of torsional vibration was eliminated by the use of a microammeter with a low period.

An assembly of monel metal slip rings bolted to the extension-shaft coupling flange and silver-graphite brushes are used as shown in figure 2 to make contacts with the bridge circuit that rotates with the shaft. The resulting sliding-contact resistance is about 1 ohm when the surfaces are clean. Because the resistance of other parts of the circuit is high, small variations in the contact resistance of the brushes has very little effect upon the results.

The strain gages used in the installation were constructed and attached as described in reference 4. Advance wire 0.0015 inch in diameter was used and each strain gage had a resistance of approximately 700 ohms. The dimensions of the strain gages are limited by the shaft size but for most installations the gages are approximately a quarter of the shaft circumference in length and 5/8 inch to 3/4 inch in width. The strain gages are placed on the shaft where they may be conveniently wired to the slip rings. A protective layer of linen tape, impregnated with a glyptal resin, is placed around the shaft covering the gages.

A schematic diagram of the complete torquemeter electrical circuit is shown in figure 3. The bridge is supplied with the required direct-current voltage by a dynamotor operating from a 12-volt battery. The current to the bridge is stabilized by connecting three iron-wire ballast tubes in series with the bridge and the dynamotor. A rheostat is provided for initial adjustment of the bridge current. Switch S_2 and rheostat R_5 are used for adjusting the zero-torque balance of the bridge. Reversing switch S_4 allows the indicating meter to be polarized for operation on either side of the balance point. The adjustment of the torque sensitivity is accomplished by inserting resistance R_8 in series with the indicating meter.

Calibration

A known torque must be applied to the shaft to calibrate the torquemeter. A static calibration was made with the engine in the airplane by removing the propeller and replacing it with a special lever arm upon which weights were hung. The engine was prevented from rotating by filling one cylinder with oil. The torque applied to the propeller shaft by the weights hung on the special lever arm divided by the gear ratio is equal to the torque delivered to the extension shaft by the engine. The sensitivity of the instrument was so adjusted that the accuracy with which it could be read was 1 percent at about 1000 horsepower. A plot of the meter reading against torque in the extension shaft is shown in figure 4. The torquemeter calibration constant as determined by static calibration was 39.0 foot-pounds torque per microampere.

A dynamic calibration to check the static calibration was made with the setup shown in figure 5. Scales were placed under the landing gear to measure the propeller-reaction torque. Zero thrust was obtained by setting two blades of the four-blade propeller at negative pitch angles. Scale tare readings were taken at frequent intervals in order that corrections for fuel consumed by the engine could be made. A comparison between static and dynamic calibrations is shown in figure 6.

As a further check, the torquemeter constant was computed from the shaft dimensions and the electrical constants of the strain gages and found to be 39.46 foot-pounds of torque per microampere. These calculations are presented in the appendix.

TESTS

Data obtained for 10 flight-test runs in which the torquemeter was used are reported. Five of these runs were made at maximum engine power and at density altitudes that ranged from about 23,000 to 31,000 feet. The other five test runs were made at a constant density altitude of about 18,900 feet with varying manifold pressure. The engine speed was measured by a calibrated sensitive tachometer. The carburetor mixture control was set at automatic-rich position for all runs.

Temperature, airspeed, altitude, and manifold pressure were automatically recorded. Observations of engine speed and torquemeter current were recorded by the pilot.

In preparation for making a test run, the airplane was flown at the desired pressure altitude and engine speed. The manifold pressure was then adjusted to the proper value (except for full-throttle runs) and flight was continued until conditions had become stabilized before data were recorded.

In addition to the flight tests two test runs were made on an Allison V-1710 engine mounted on a dynamometer test setup and equipped with an identical supercharger. The conditions of carburetor inlet-air pressure, temperature, and exhaust pressure were adjusted for NACA standard atmosphere at 17,000 and 29,000 feet. The maximum power output of the engine at 3000 rpm was measured by an electric absorption dynamometer.

RESULTS AND DISCUSSION

The density altitudes at which the flight tests were made were determined by first computing the air density corresponding to the observed pressure and temperature. The altitude in feet corresponding to this density in the standard atmosphere (reference 5) was then taken as the density altitude for the test.

The engine brake horsepower was calculated from torquemeter data by the equation

$$\text{bhp} = K_1 K_2 N I$$

in which

K_1 $\quad \dfrac{2\pi}{33,000}$

K_2 39.0 foot-pounds per microampere

N engine speed, rpm

I meter current, microamperes (corrected)

In the correction of the observed torquemeter current, the zero reading taken immediately after each flight was used for corresponding data because it was believed to be representative of the stabilized condition of the bridge.

The comparison of the power output of the engine in the full-power tests at different density altitudes is shown in figure 7. Good agreement exists between the power measured in flight and the engine manufacturer's full-throttle calibration line (maximum available power), which is included for comparison. No attempt has been made to correct the measured power for differences in temperature and pressure at the supercharger outlet under the test conditions and under the calibration conditions.

The test points for the simulated altitude tests are also shown. The power at a simulated altitude of 29,000 feet was 932 brake horsepower and the power measured in flight at a density altitude of 28,970 feet was 907 brake horsepower.

The power output of the engine in the tests at constant density altitude with variable manifold pressure is shown in figure 8. Comparable data, taken from the engine manufacturer's calibration chart, are also shown. The difference between the manifold pressures measured in flight and those taken from the chart for like powers indicates the desirability of measuring engine power under actual flight conditions. These differences are usually the result of such installation factors as jet exhaust stacks, air-scoop effects on carburetor calibrations, air conditions other than standard at the carburetor inlet, and manual control of equipment intended to be automatic, such as auxiliary stage supercharger. These factors may cause the engine operating conditions to differ from the calibrations determined on the altitude test stand with standard NACA altitude at both engine inlet and exhaust.

Constancy of the electrical zero of the torquemeter may be considered to be an indication of the stability of the calibration of the apparatus. The electrical zero did not vary more than 2 microamperes during the tests and no readjustment of the bridge balance was made. Figure 6 shows that the variation between the static and the dynamic calibrations is within ±2 percent.

SUMMARY OF RESULTS

Flight measurements with an electric strain-gage torquemeter of the power output of an Allison V-1710-93 engine were in good agreement with the values shown by the engine manufacturer's calibration chart on the basis of maximum available horsepower at altitudes above 20,000 feet. The measured values of manifold pressure for the reduced power runs at a density altitude of 18,900 feet were higher for a given horsepower than indicated by the manufacturer's calibration chart.

The electric torquemeter was found to be a reliable instrument for determining engine power output in flight. The accuracy is shown to be within ±2 percent by three calibration methods. The readings and manipulations required of the pilot consist in selecting the proper polarity and reading the meter.

Aircraft Engine Research Laboratory,
National Advisory Committee for Aeronautics,
Cleveland, Ohio.

APPENDIX

CALCULATION OF TORQUEMETER CONSTANT

The following symbols are used for calculations:

I_o meter circuit current, amperes

I_m meter current, amperes

E_v applied voltage, volts

K strain-gage constant, 2

T torque, in.-lb

r shaft radius, in.

μ Poisson's ratio

J polar moment of inertia, $(\text{in.})^4$

E Young's modulus of elasticity, lb/sq in.

σ stress, lb/sq in.

ϵ strain $\Delta l/l$, in./in.

R gage resistance, ohms

R_m meter resistance, ohms

R_f fuse resistance, ohms

R_s series resistance with meter, ohms

R_d shunt resistance with meter, ohms

The strain sensitivity for a resistance-wire strain gage, as defined in reference 4, is the ratio of the proportional increase in resistance $\Delta R/R$ to the strain $\Delta l/l$, giving a gage constant

$$K = \frac{\Delta R/R}{\Delta l/l}$$

where K has been determined experimentally as 2.0.

In a Wheatstone bridge circuit the meter current I_o, as determined in reference 6, is

$$I_o = \frac{(R_2R_3 - R_4R_1)\ E_v}{R_1R_2R_3 + R_2R_3R_4 + R_3R_4R_1 + R_4R_1R_2 + R_m(R_1 + R_2)(R_3 + R_4)}$$

When the gages, as shown in figure 3, are subjected to a torsional stress in such a way that R_1 and R_4 increase because of elongation and R_2 and R_3 (placed 90° to R_1 and R_4) contract, the strain ϵ in each case is due to a direct stress effect and a Poisson's ratio effect. In reference 7 it is shown that

$$\epsilon_4 = \epsilon_1 = \frac{\sigma}{E}(1 + \mu)$$

also

$$\epsilon_2 = \epsilon_3 = -\frac{\sigma}{E}(1 + \mu)$$

In a balanced bridge circuit where $R_1 = R_2 = R_3 = R_4$

$$R_1 \text{ and } R_4 = R(1 + K\epsilon)$$

$$R_2 \text{ and } R_3 = R(1 - K\epsilon)$$

$$I_o = \frac{\left[R^2 (1 - K\epsilon)^2 - R^2 (1 + K\epsilon)^2\right] E_v}{R^3 \left[2 (1 + K\epsilon)(1 - K\epsilon)^2 + 2 (1 + K\epsilon)^2 (1 - K\epsilon)\right] + 4R_mR^2}$$

$$= \frac{E_v(1 - 2\ K\epsilon + K^2\epsilon^2 - 1 - 2\ K\epsilon - K^2\epsilon^2)}{2R\ (1 + K\epsilon)(1 - K\epsilon)(1 + K\epsilon + 1 - K\epsilon) + 4R_m}$$

Collecting terms,

$$I_o = \frac{E_v(-4K\epsilon)}{4R\ (1 - K^2\epsilon^2) + 4R_m}$$

if $K^2\epsilon^2$ is small then,

$$I_o = \frac{E_v K\epsilon}{R + R_m}$$

Since $\epsilon = \frac{\sigma}{E}(1 + \mu)$ and $\sigma = \frac{Tr}{J}$

$$\epsilon = \frac{Tr}{JE}(1 + \mu)$$

Substituting in the equation for ϵ and adding resistances effective to the meter circuit, I_o becomes

$$I_o = \frac{E_v KT\ r\ (1 + \mu)}{JE\ (R + R_m + R_f + R_s)}$$

Substituting the proper values

$$I_o = \frac{105 \times 2 \times T \times 1.25\ (1 + 0.25)}{12\pi\ \frac{\left[(1.25)^4 - (1.09374)^4\right]}{2} \times 30 \times 10^6 \left(700 + \frac{15{,}000 \times 1775}{15{,}000 + 1775} + 125 + 500\right)}$$

$= 0.02835$ microampere/ft-lb

Because the meter is dampened with a shunting resistor

$$I_m = \frac{I_o R_s}{R_m + R_d}$$

$$= \frac{0.02835 \times 15{,}000}{1775 + 15{,}000}$$

$= 0.02535$ microampere/ft-lb

or

39.46 ft-lb/microampere

REFERENCES

1. Gagg, R. F., and Farrar, E. V.: Altitude Performance of Aircraft Engines Equipped with Gear-Driven Superchargers. SAE Trans., vol. 34, no. 6, June 1934, pp. 217-223.

2. Bikle, Paul F.: Performance Flight Testing Methods in Use by the Flight Section. A.C.T.R. No. 5069, Army Air Forces, Materiel Command, Jan. 15, 1944.

3. de Forest, A. V., and Leaderman, H.: The Development of Electrical Strain Gages. NACA TN No. 744, 1940.

4. Nettles, J. Cary, and Tucker, Maurice: Construction of Wire Strain Gages for Engine Application. NACA ARR No. 3L03, 1943.

5. Diehl, Walter S.: Standard Atmosphere---Tables and Data. NACA Rep. No. 218, 1925 (reprint 1942).

6. Michels, Walter C.: Advanced Electrical Measurements. D. Van Nostrand Co., Inc. (New York), 2d ed., 1941, pp. 16-17.

7. Timoshenko, S.: Theory of Elasticity. McGraw-Hill Book Co., Inc., 1934. p. 9.

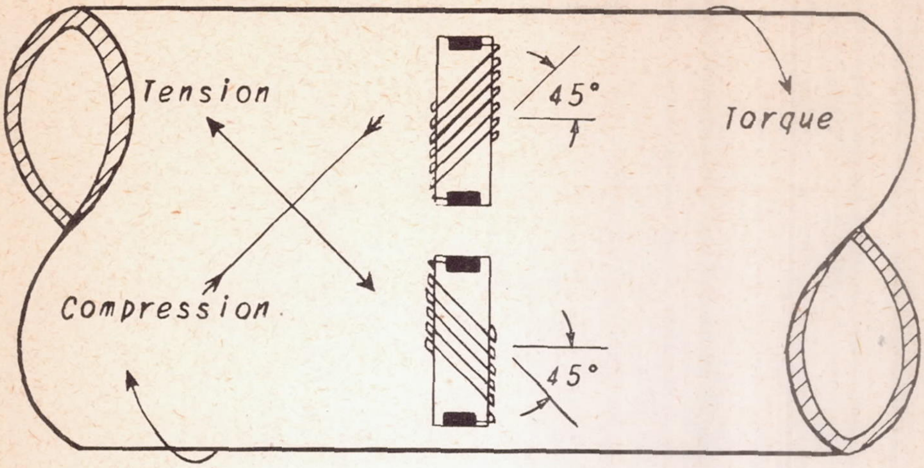

(a) Location of wire strain gages for measuring torsional strains.

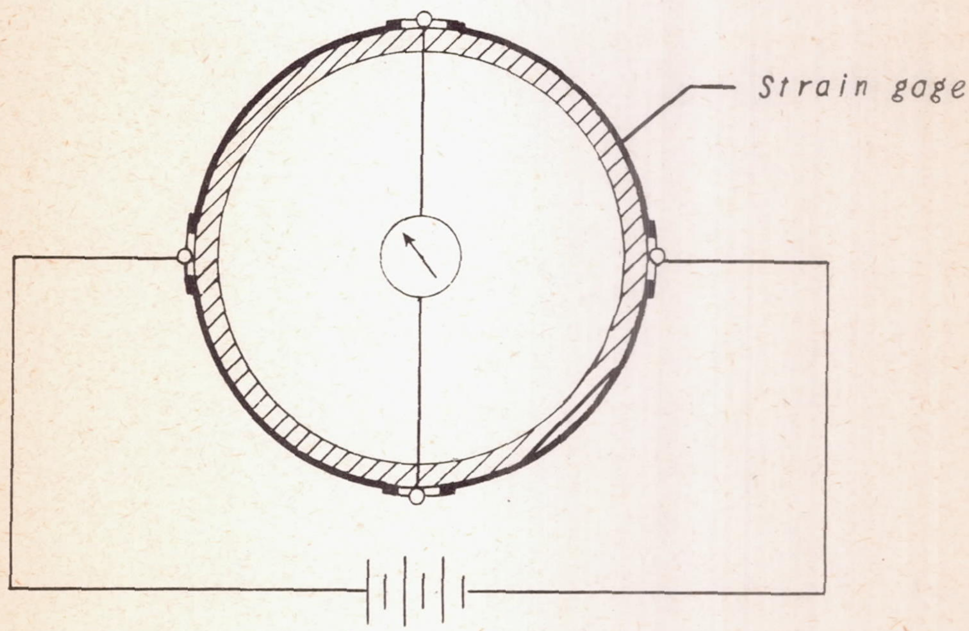

(b) Schematic diagram of strain-gage bridge on shaft.

NATIONAL ADVISORY
COMMITTEE FOR AERONAUTICS

Figure 1. - Arrangement of the NACA electric torquemeter strain gages on a shaft.

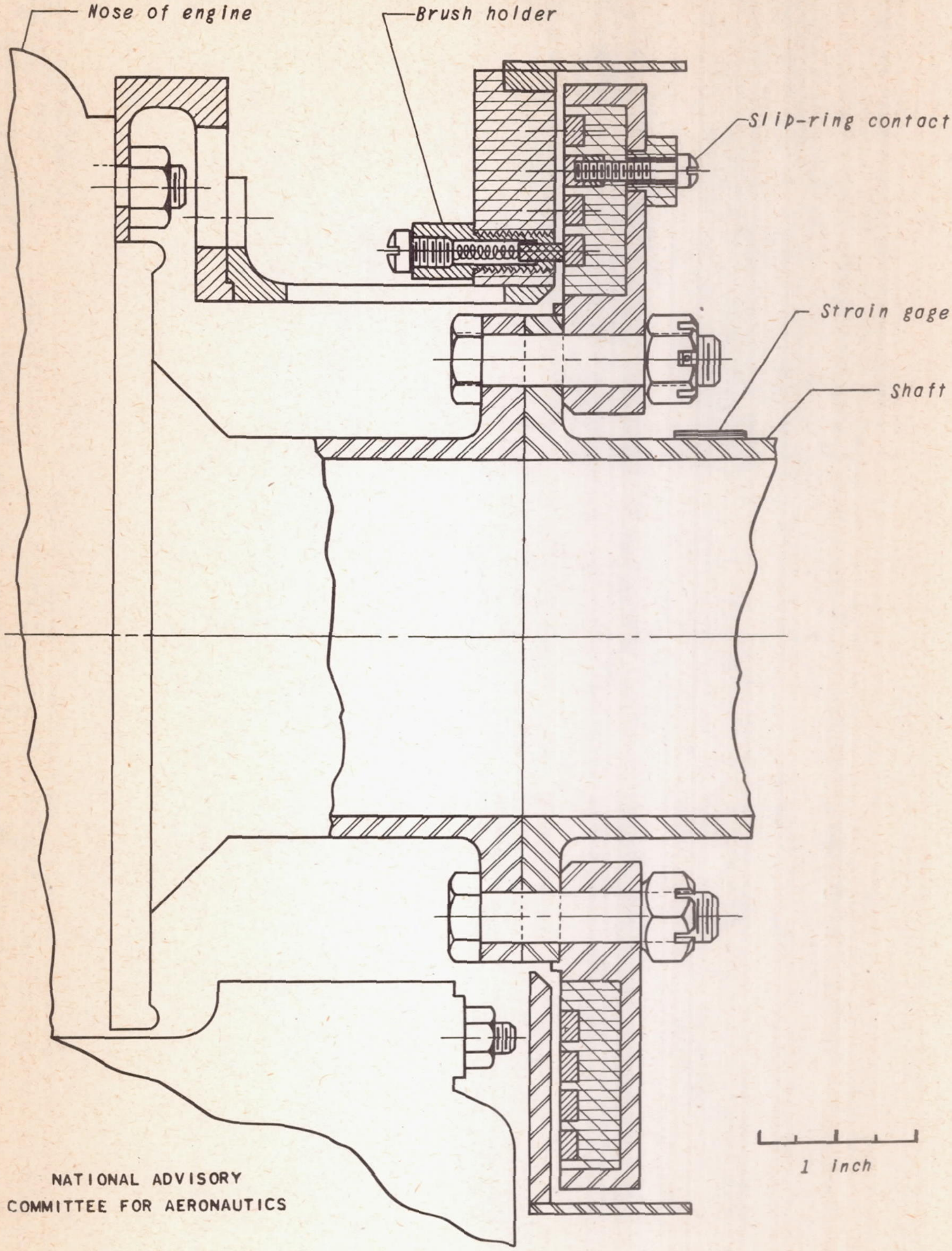

Figure 2. - Torquemeter slip rings and brushes installed on the engine.

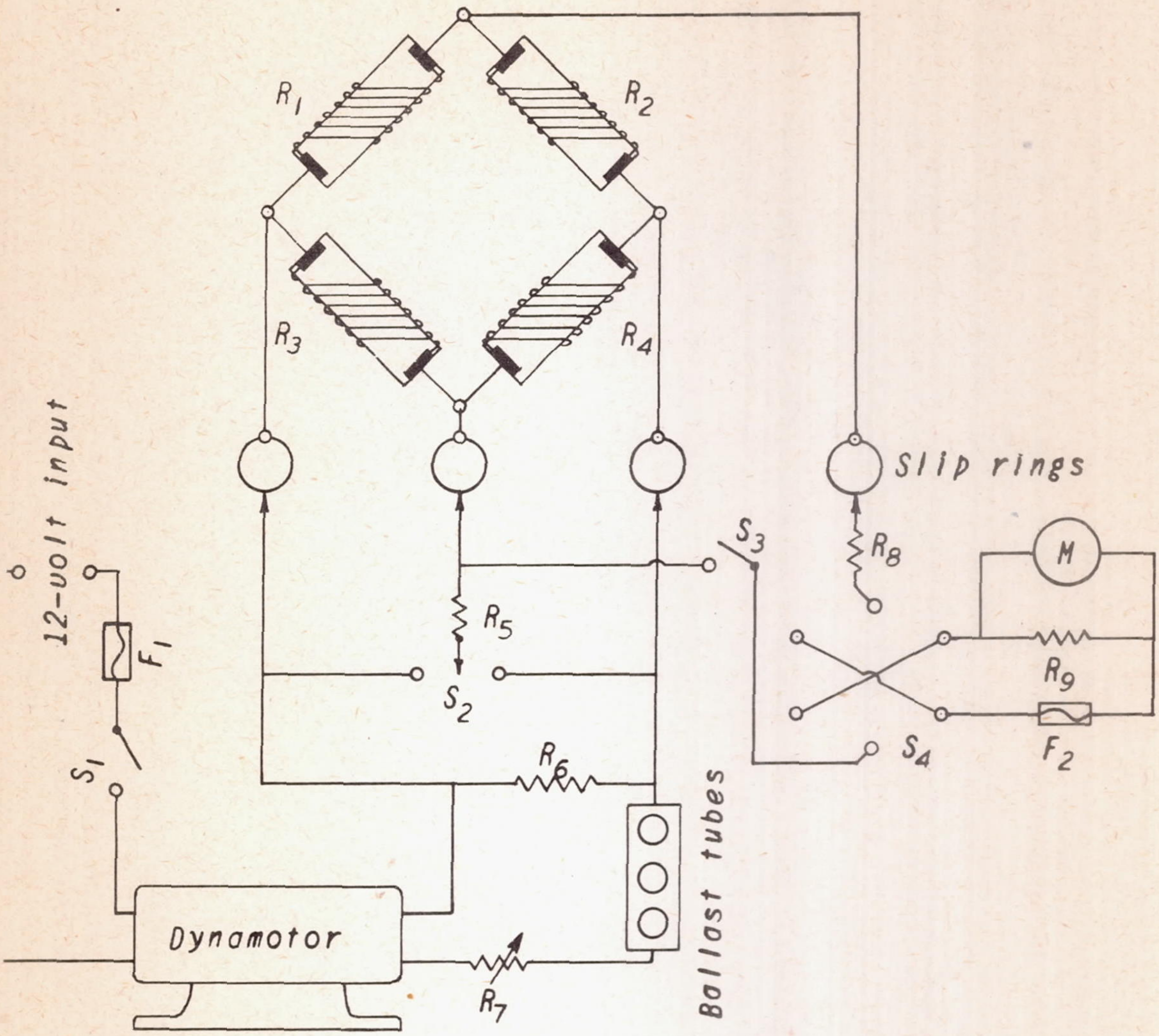

S_1 Power switch
S_2 Balancing resistor switch
S_3 Meter switch
S_4 Meter reversing switch
R_1, R_2, R_3, R_4 Strain gages
R_5 Rheostat-balancing resistor
R_6 Bridge shunting resistor
R_7 Current regulator
R_8 Series-meter resistor
R_9 Meter-damping resistor
F_1 Supply fuse (5 amperes)
F_2 Meter fuse (2 milliamperes)
M Meter

Figure 3. - Schematic circuit diagram of NACA electric torquemeter.

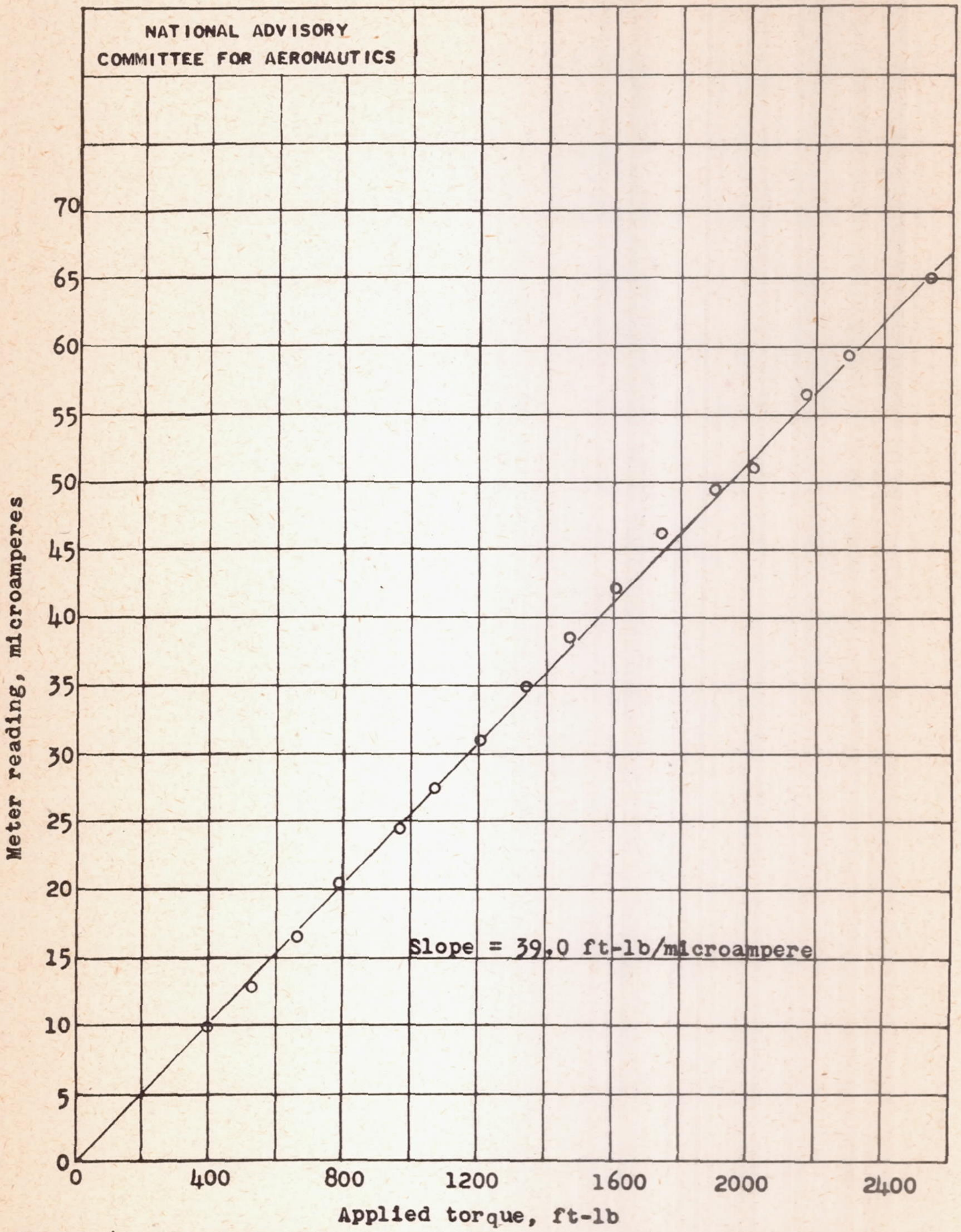

Figure 4.- Static calibration curve of the electric torquemeter. Bell P-63A-1 airplane; Allison V-1710-93 engine.

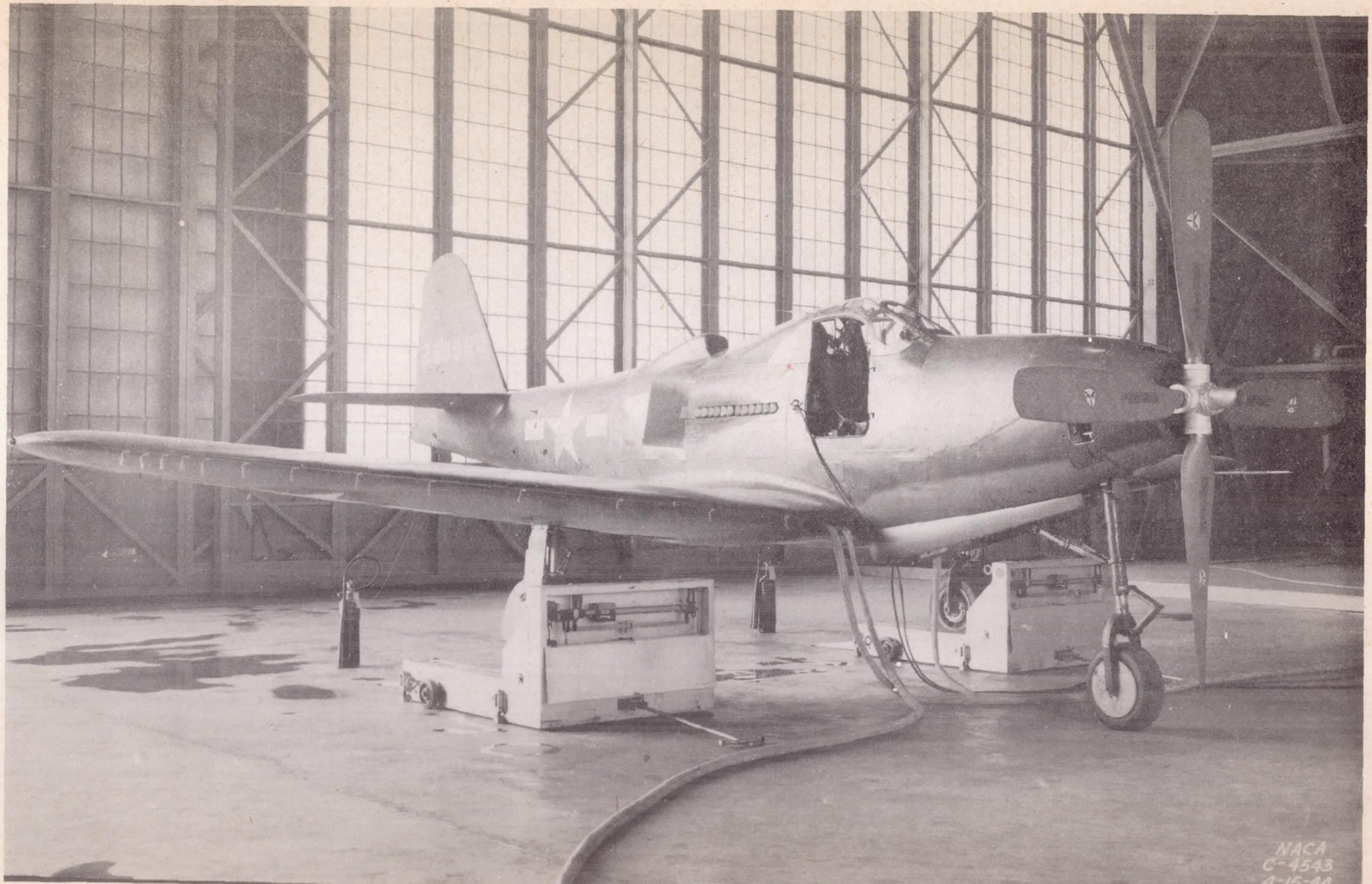

Figure 5. - Test setup for the dynamic calibration of the NACA electric torquemeter. Allison V-1710-93 engine; Bell P-63A-1 airplane.

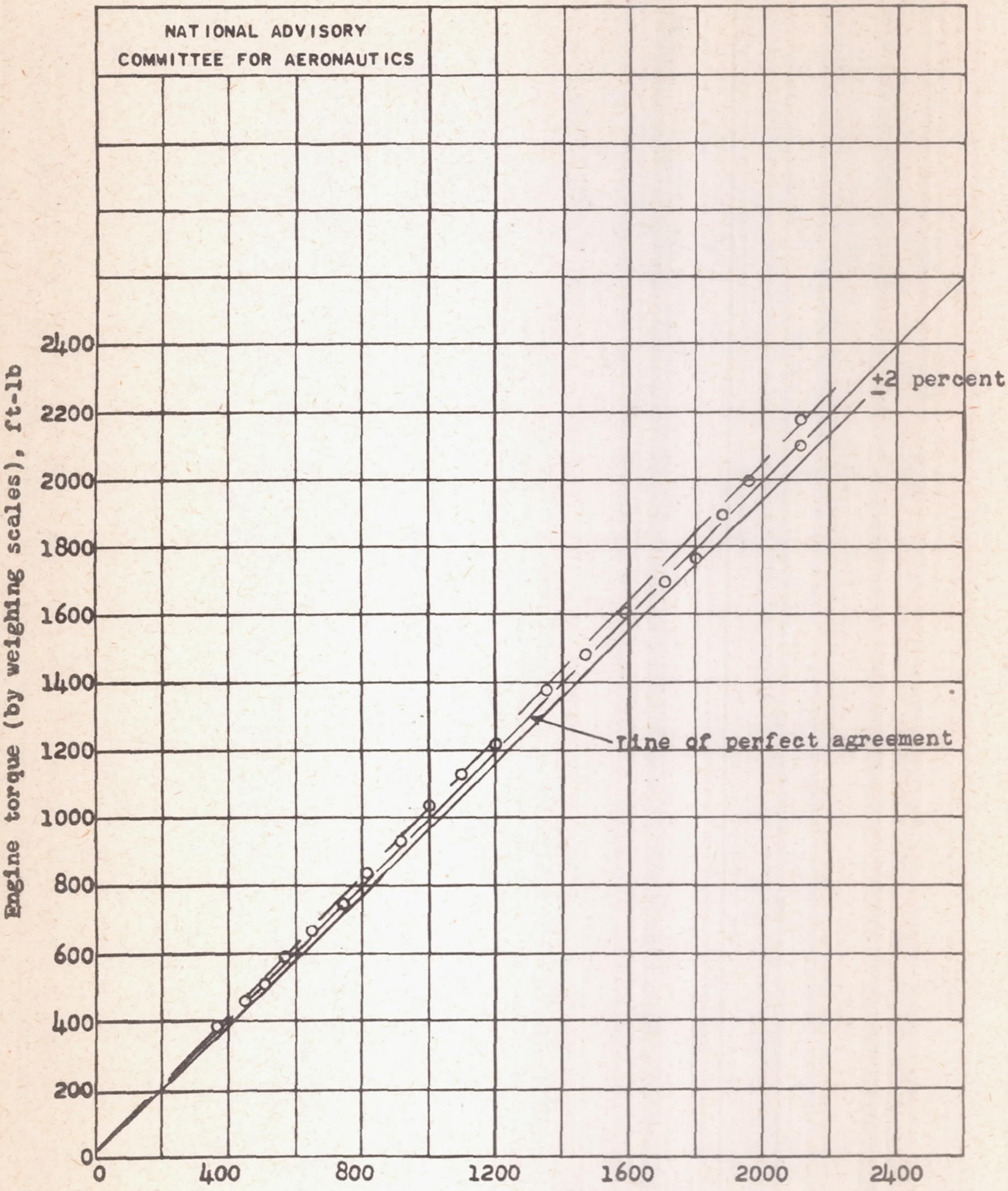

Figure 6.- Comparison between torque values as determined by propeller reaction and electric torquemeter constant as determined by static calibration. Bell P-63A-1 airplane; Allison V-1710-93 engine; engine speed and power varied according to propeller load.

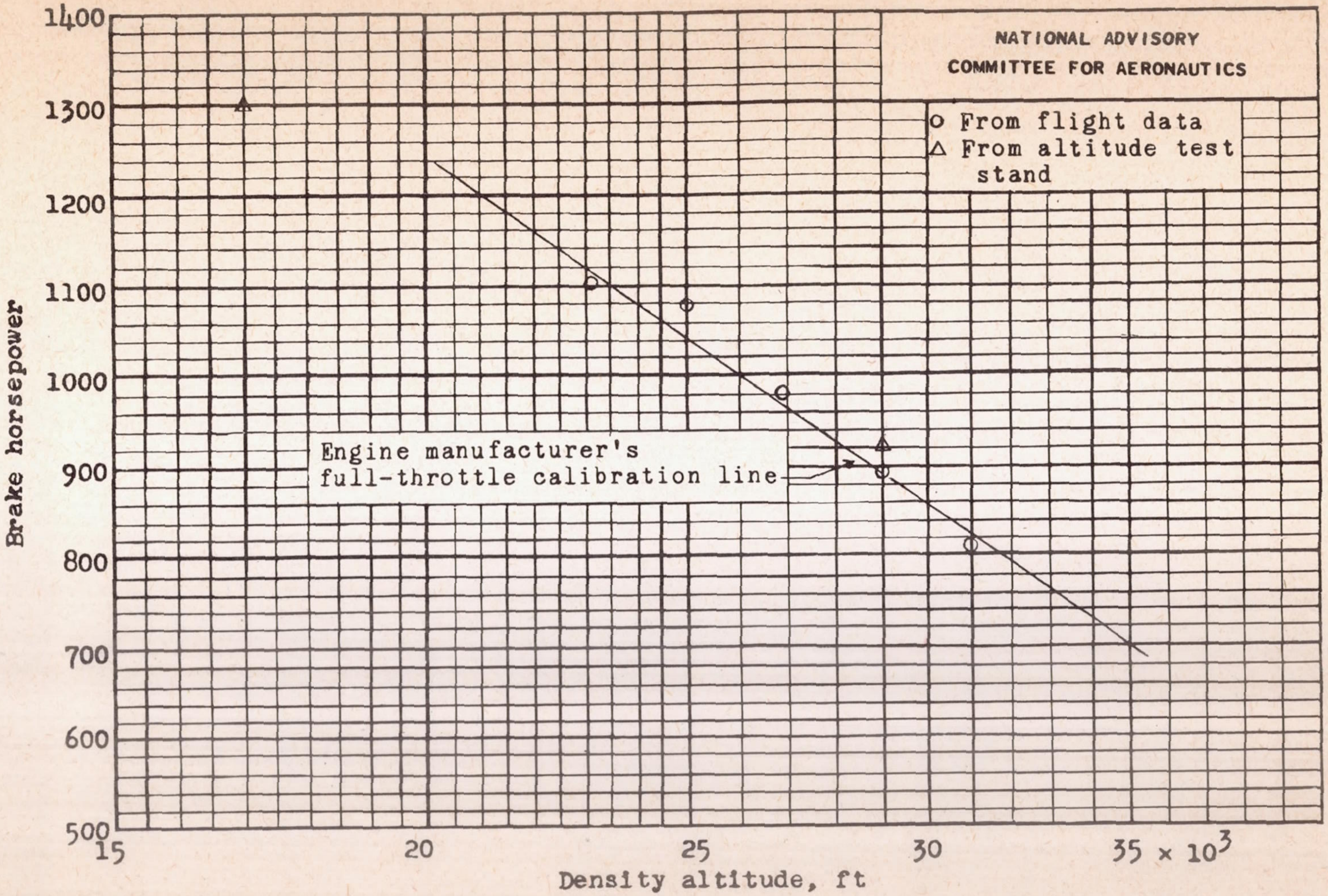

Figure 7.- Comparison of altitude performance of the Allison V-1710-93 engine as determined by torquemeter in flight in the Bell P-63A-1 airplane, altitude test stand, and engine manufacturer's calibration chart. Engine speed, 3000 rpm; full throttle; maximum auxiliary supercharger speed; mixture setting, automatic rich.

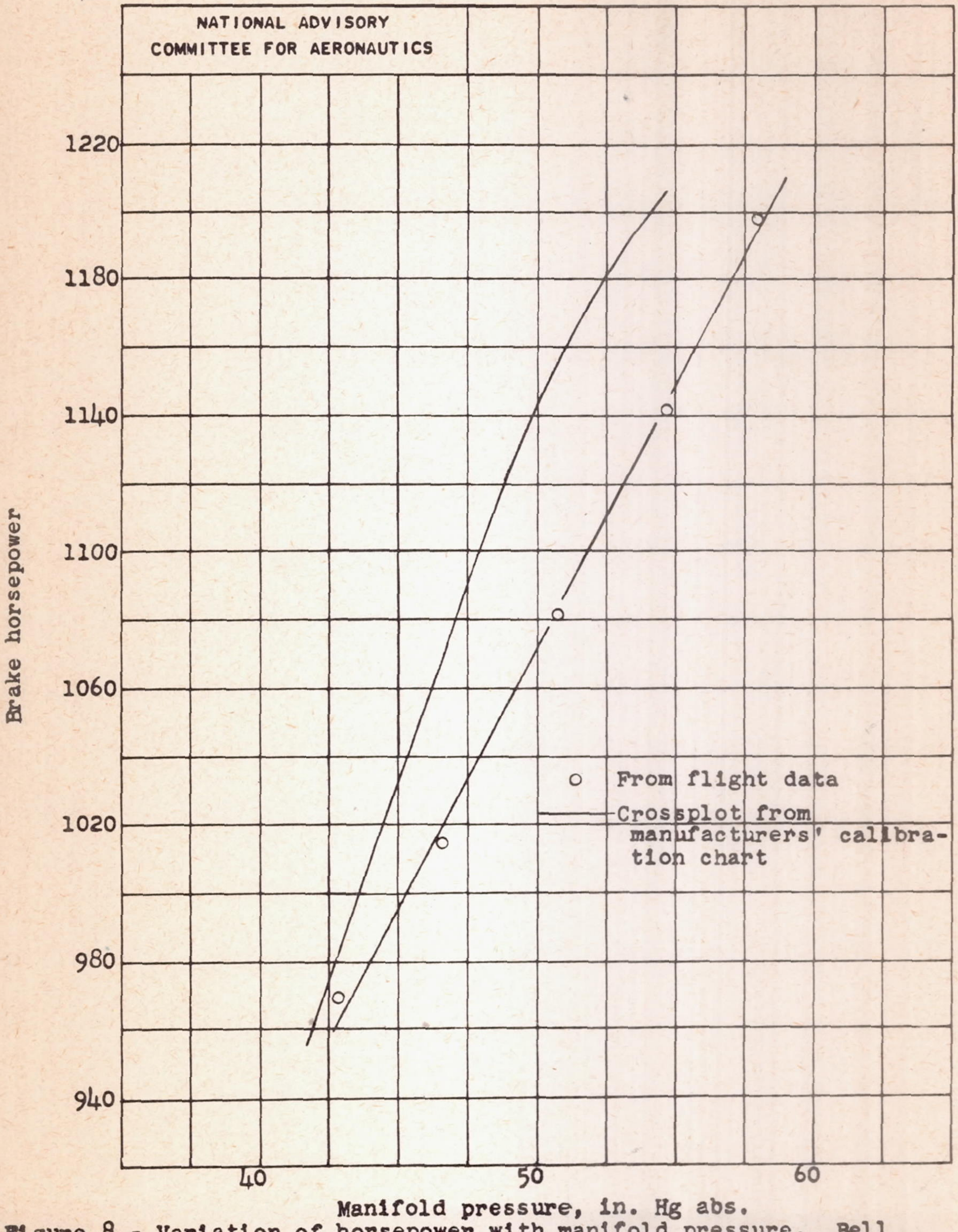

Figure 8.- Variation of horsepower with manifold pressure. Bell P-63A-1 airplane; Allison V-1710-93 engine; engine speed, 3000 rpm; density altitude, 18,900 feet; mixture setting, automatic rich.